RSC Advances

PAPER

View Article Online
View Journal | View Issue

Cite this: *RSC Adv.*, 2021, **11**, 1984

The combination of Al_2O_3 and BN for enhancing the thermal conductivity of PA12 composites prepared by selective laser sintering

Yue Yuan,[a] Wei Wu, *[a] Huanbo Hu,[b] Dongmei Liu,[b] Hui Shen[a] and Zhengyi Wang[a]

A powder-based 3D printing technology, selective laser sintering (SLS), is a novel strategy of manufacturing complex components with specially tailored properties, including mechanical properties, as well as thermal and electrical conductivity. In this study, the effect of incorporating Al_2O_3 particles and BN plates on the thermal conductivity of PA12 composites was investigated. PA12 composite powders, which can be well applied to SLS, were prepared *via* a two-step approach to mixing. Morphology characteristics demonstrated that the fillers dispersed uniformly in the PA12 matrix, as expected. With 35 wt% Al_2O_3 and 15 wt% BN hybrid fillers, the tensile strength had the potential to reach 25.7 MPa, while the thermal conductivity could reach 1.05 W m^{-1} K^{-1}, 275% higher than that of pure PA12. In addition, the study investigated the effects of filler content on the thermal stability and mechanical properties whilst analysing the melting and crystallisation behaviours of SLS components. The results demonstrate that these composites have favourable thermal stability and exhibit no severe deterioration in mechanical properties. The PA12 composites prepared in this work therefore illustrated vast potential in thermal management materials.

Received 18th November 2020
Accepted 23rd December 2020

DOI: 10.1039/d0ra09775f

rsc.li/rsc-advances

1 Introduction

Currently, due to the rapid development of science and technology, there are increasing demands for thermal management materials.[1–3] Consequently, thermally conductive polymer composites have attracted widespread attention due to their excellent properties, two of which include being lightweight and processable.[4] As a result more refined, yet complicated, methods to develop thermally conductive components, compression and injection moulding, as well as other traditional processing technologies, have been rendered inadequate in the production of thermally conductive polymer composites with highly complex shapes.[5] Additive manufacturing is an emerging technology used for the production of engineering materials.[6,7] Selective laser sintering (SLS) is currently one of the most promising 3D printing technologies, based on the basic principle of high-temperature sintering of powder materials under laser irradiation.[8,9] When compared with traditional manufacturing methods, SLS technology demonstrates greater advantages in the fabrication of materials with complex shapes and high precision.[10]

With excellent mechanical properties and good thermal stability establishing it as an effective component for the 3D printing of raw materials,[11,12] polyamide 12 (PA12) is one of the most widely utilised engineering plastics, applied to electronics and the automotive industry.[13] The intrinsic thermal conductivity of PA12 is, however, only about 0.28 W m^{-1} K^{-1}, thus cannot meet the requirements for higher thermal conductivity in the field of thermal management materials. There have been several successful studies on the thermal conductivity of PA12 composites fabricated by selective laser sintering. For example, Yang *et al.*[14] prepared PA12/BN composites *via* the solid-state shear milling method, identifying that, with 40 wt% BN loading, the thermal conductivity could reach 0.55 W m^{-1} K^{-1}. Lanzl *et al.*[9] first chose to investigate the thermal conductivity of PA12 composites filled with copper particles, which elicited little significant change in the thermal conductivity as a result of the increased filler content. Yuan *et al.*[15] used the content of 0.1, 0.5, and 1 wt% carbon nanotubes for filling PA12, obtaining a maximum thermal conductivity of just 0.4 W m^{-1} K^{-1} in this experiment. In these prior studies, the improvement of PA12 composites' thermal conductivity was not evident. On the one hand, as selective laser sintering is a near zero-shear-rate layered manufacturing process, the thermally conductive filler is prone to separation by the polymer matrix, therefore making it difficult for the filler to form an effective thermal network during this process. On the other hand, however, a large volume of single filler is often required to obtain high thermally conductive polymer composites. In order to ensure the fluidity of the composite powder and mechanical properties of

[a]*Sino-German Joint Research Center of Advanced Materials, School of Materials Science and Engineering, East China University of Science and Technology, Shanghai, 200237, PR China. E-mail: wuwei@ecust.edu.cn*
[b]*Oechsler Plastic Products (Taicang) Co., Ltd., Suzhou 215000, PR China*

the sintered samples, the amount of thermally conductive filler must be controlled within a certain range. It is thus necessary to identify an alternative approach to improve thermal conductivity with relatively low filler content.

To improve the thermal conductivity of polymer composites whilst reducing the filler content during traditional processing methods, combining a range of fillers with various shapes have been noted as effective. The hybrid fillers promote the formation of more efficient heat conduction paths, compared to those created with just a single filler. Much research has been conducted focusing on the synergistic effect of hybrid fillers, with Mai *et al.*[16] studying the thermal conductivity of epoxy resins filled with a mixture of Al_2O_3 and BN. The results identified that the orientation of BN plates was conducive to the formation of higher thermally conductive pathways. Chen *et al.*,[17] meanwhile, utilised spherical Al_2O_3 to construct three-dimensional graphene foam. Under the influence of spherical alumina, the graphene exhibited a synergistic effect in the enhancement of composites' thermal conductivity. In previous work, a novel hybrid filler, comprising of boron nitride and copper, was successfully prepared, which was found due to the introduction of the Cu to encourage increased rates of thermal conductivity compared to with just a single filler.[18] This research, therefore, sought to extend the steps made in prior studies, introducing two distinct, thermally conductive fillers into the fabrication of PA12 composites *via* selective laser sintering. Due to its low cost and excellent insulation properties, Al_2O_3 has been widely applied to enhance the thermal conductivity of composites.[19,20] BN has a two-dimensional lamellar structure that is similar to graphite, with a thermal conductivity reaching as high as 300 W m^{-1} K^{-1} in the direction parallel to the crystal plane.[21] The combined use of Al_2O_3 and BN can exert a synergistic effect on the thermal conductivity of the composites, because the BN can be used as a heat conduction channel in the polymer matrix, while the Al_2O_3 particles contact the BN surface to construct more thermally conductive networks, thereby reducing the interface thermal resistance and effectively improving the thermal conductivity of the composites.

In this paper, powder-based 3D printing technology was incorporated to prepare high thermal conductivity parts in combination with complex geometries. For the first time, two dissimilar thermally conductive fillers were selected to prepare PA12 composites with high thermal conductivity *via* selective laser sintering, with the expectation that the bridging of BN plates and Al_2O_3 particles would aid the formation of more thermally conductive networks in the polymer matrix. The surface morphology, thermal conductivity, and the thermal conductivity improvement mechanism of PA12 composites were subsequently investigated. Additionally, the crystallisation behaviours, thermal stability, and mechanical properties of the composites were also studied. This work demonstrates that the introduction of hybrid fillers in SLS technology is an effective method for the manufacture of thermally conductive polymer composites with high thermal conductivity, complex structures, and good mechanical properties.

2 Experimental section

2.1. Materials

PA12 powder (10–100 μm, 1.03 g cm^{-3}), adopted as the polymer matrix of the composites, was purchased from Hunan Farsoon High-Technology Co., Ltd. Hexagonal boron nitride (h-BN, 10–15 μm, 2.35 g cm^{-3}) and spherical alumina (Al_2O_3, 5–10 μm, 3.90 g cm^{-3}) were both supplied by Qinhuangdao Eno High-Tech Material Development Co., Ltd.

2.2. Preparation of PA12 composite powder

The PA12 composites were prepared *via* a two-step mixing approach.

First, the dried PA12 powder was alternately mixed with variable ratios of Al_2O_3 and BN using a high-speed mixer for 1 h. Following this, the resulting mixture was thoroughly blended by ball milling for 4 h. The SLS experiments were performed on a HT 252P commercial SLS machine (Hunan Farsoon High-Technology Co, Ltd.) with a continuous wave CO_2 laser. The schematic diagram of the SLS process was illustrated in Fig. 1(a). The sintering parameters used in this study were as follows: laser power 45–50 W; laser scan speed 7600–10 160 mm s^{-1}; powder layer thickness 0.1 mm; scan spacing 0.15–0.3 mm; powder preheating temperature 170–175 °C. Specific processing parameters of some samples were shown in Table 1. Energy density (ED) is defined as the energy of the laser acting on per unit area, and the calculation is as follows:

$$\mathrm{ED} = \frac{P}{H \times v} \quad (1)$$

where P is the laser power, H is the scan spacing, v is the laser scan speed. To prevent the oxidisation of the raw powder, an atmosphere containing less than 5% oxygen was required for the 3D printing process. The sintered samples remained in the machine following the sintering process, until the chamber reached below 80 °C, with the entire SLS process lasting approximately 3 h. As illustrated in Fig. 1(b), the sintered samples of PA12 composites were successfully prepared.

2.3. Characterization

The morphology of the powders and the fracture surface of the sintered parts were observed by a scanning electron microscopy (SEM, JCM-6000, Japan) with an acceleration voltage of 5 kV.

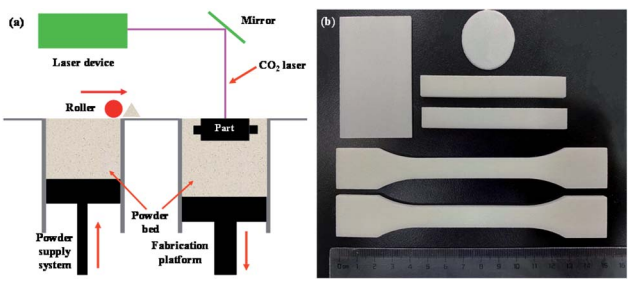

Fig. 1 (a) Schematic diagram of SLS process and (b) the sintered samples of PA12 composite at 45 wt% Al_2O_3 + 5 wt% BN loading.

Table 1 Processing parameters used for the fabrication of PA12 composites

Parameters	PA12	PA12/30Al_2O_3	PA12/50Al_2O_3	PA12/35Al_2O_3/15BN
Laser power (W)	45	50	50	50
Scan speed (mm s^{-1})	10 160	10 160	10 160	8800
Scan spacing (mm)	0.30	0.30	0.25	0.15
Layer thickness (mm)	0.1			
Bed temperature (°C)	170.5	170.5	171.0	174.0
ED (J mm^{-2})	0.0148	0.0164	0.0197	0.0379

Prior to observation, each sample was frozen in liquid nitrogen, then fractured and coated with a conductive gold layer in the vacuum chamber. X-ray diffraction (XRD) analysis was measured by an Ultima IV X-ray diffractometer using Cu Kα radiation with a 2θ range of 10°–80° at a scan rate of 4° per minute. The thermal conductivity of the samples was measured by the thermal conductivity instrument TC3000E at room temperature. In this method, every sample was polished to a dimension of 60 mm × 40 mm × 2 mm and tested individually five times. Thermal gravimetric analysis (TGA) was carried out on the TA Q50 instrument from room temperature to 750 °C at a heating rate of 10 °C min^{-1} under a nitrogen atmosphere. The melting and crystallisation behaviours of the composites were determined by the differential scanning calorimetric (PerkinElmer Instruments, USA). First, the samples were heated from 25 °C to 220 °C, at a rate of 10 °C min^{-1} under a nitrogen atmosphere, and held for 5 minutes to eliminate the thermal history. These samples were subsequently cooled to 25 °C at a rate of 10 °C min^{-1} to obtain the crystallisation curves. A universal testing machine (CMT 4204) was utilised to perform tensile tests, adhering to the GB/T1040-2006 standard, at a cross-head rate of 10 mm min^{-1}.

3 Results and discussion

3.1. Characterisation of PA12 composite powder

Fig. 2 shows the SEM images of BN and Al_2O_3 particles. With an average size of 5–10 μm, the spherical morphology of the Al_2O_3 particles can be well applied to SLS. The obtained XRD pattern of the Al_2O_3 particles corresponds to the XRD pattern of α-Al_2O_3, indicating that the Al_2O_3 used is α-Al_2O_3, which has better thermal conductivity than other crystal forms of Al_2O_3.[22] The results demonstrate that BN has a typical two-dimensional layered structure with a diameter of 10–15 μm. Both surfaces of BN and Al_2O_3 particles are smooth. In Fig. 2(e), where the XRD curve of BN is visible, the characteristic peaks of BN can be observed, with almost no other peaks identifiable, which indicates the purity of the BN used in the experiment.[23] Fig. 2(c) presents the morphology of the PA12 composite powders. The PA12 powder has a relatively regular spherical shape, with particle size ranging from 10 to 100 μm, both of which allow the powder to have good fluidity and processability, thus making it easy for powder spreading and 3D printing.[24] It can be observed that the Al_2O_3 and BN are both uniformly dispersed in the PA12 matrix without agglomeration. Furthermore, the close contact of Al_2O_3 and BN allows for the formation of continuous thermal networks, essential for the improvement of thermal conductivity. It is worth noting that a few fillers are embedded into the PA12 matrix due to the strong shear force of the ball milling equipment. This is beneficial to the improvement of interface compatibility between fillers and the PA12 matrix, as well as the dispersion of fillers in the matrix. As can be identified from Fig. 2(f), pure PA12 exhibits two diffraction peaks at 2θ = 20° and 23.7°. Following the blending with fillers, the emergence of a series of diffraction peaks corresponding to the XRD pattern of BN and Al_2O_3 indicates that the PA12 composite powders were correctly and successfully prepared.

3.2. Thermal conductivity of composites

Fig. 3(a) illustrates the thermal conductivity of the sintered PA12 composites with a single filler, where it can be noted that, with the increase of Al_2O_3 loading, there is a distinct

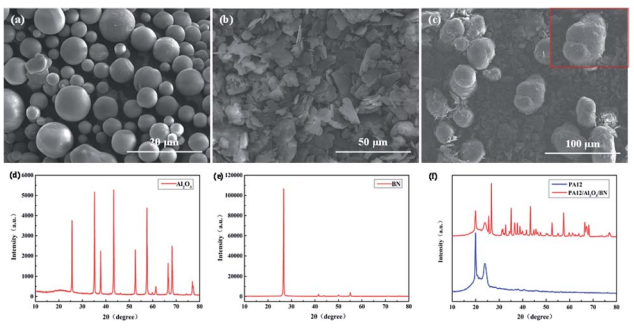

Fig. 2 SEM images of (a) Al_2O_3, (b) BN and (c) PA12/Al_2O_3/BN composite at 30 wt% Al_2O_3 + 20 wt% BN loading. X-ray diffraction (XRD) curves of (d) Al_2O_3, (e) BN and (f) PA12/Al_2O_3/BN composite.

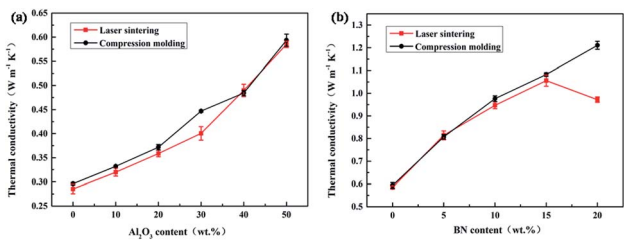

Fig. 3 Thermal conductivity of (a) PA12/Al_2O_3 and (b) PA12/Al_2O_3/BN composites as a function of BN content (with total filler content of 50 wt%).

improvement in the thermal conductivity of PA12/Al_2O_3 composites in comparison with pure PA12. The thermal conductivity of the sintered samples comes up to 0.58 W m^{-1} K^{-1} with 50 wt% Al_2O_3 loading, which is twice as high as that of pure PA12. At a low filler content, the Al_2O_3 particles are separated by the PA12 matrix, leading to low thermal conductivity. With the increase of Al_2O_3 content, the Al_2O_3 particles were increasingly likely to come into contact with each other to form thermally conductive networks throughout the polymer matrix, promoting the conduction of heat and, therefore, higher thermal conductivity. The pressure-free nature of the laser sintering process inevitably leads to the formation of voids in the sintered samples during SLS processing.[25] As a result, the thermal conductivity of the compression-moulded samples is slightly higher than that of the SLS sintered samples.

An investigation consisting of combining Al_2O_3 and BN was carried out in order to further improve the thermal conductivity and decrease the filler content. The maximum filler content was set as 50 wt%, as adding excessive filler content will significantly reduce the fluidity of the composite powder, which is unfavourable for selective laser sintering. As illustrated in Fig. 3(b), the thermal conductivity of PA12/Al_2O_3/BN composites comes up to 1.05 W m^{-1} K^{-1} when the content of BN reaches 15 wt%, approximately 275% higher than that of pure PA12, and 81% higher than the PA12/Al_2O_3 composite with an equivalent filler loading. Due to its graphite-like flat surface and high thermal conductivity, BN can be used as a heat conduction channel to connect Al_2O_3 particles, allowing the formation of more thermally conductive networks, thereby improving the thermal conductivity. However, there is a distinct decrease in the thermal conductivity when the loading of BN increases from 15 wt% to 20 wt%, which can be attributed to BN's tendency to create voids and defects during the powder spreading process, resulting from its two-dimensional layered structure, the rapid laser irradiation process fails to thoroughly eliminate this tendency. These many voids and defects in the PA12/Al_2O_3/BN composites can potentially form considerable interface thermal resistance and result in severe phonon scattering, thereby reducing the thermal conductivity. In contrast, the thermal conductivity of the compression-moulded PA12/Al_2O_3/BN composites demonstrates no decline with the increase of BN content.

3.3. Morphology and thermal conduction mechanism of composites

Fig. 4(a–d) presents the SEM images of PA12/Al_2O_3 powder. It can be seen that, at a low content, Al_2O_3 is uniformly dispersed in the PA12 matrix and the Al_2O_3 particles are separated by the PA12 matrix. The Al_2O_3 particles begin to connect and form heat conduction paths with the addition of 50 wt% Al_2O_3. Nevertheless, large gaps remain among the Al_2O_3 particles, which reduces the enhancement of thermal conductivity. It is worth noting that pure PA12 with three-dimensional structure disperses uniformly during the powder spreading process. While the Al_2O_3 loading comes up to 50 wt%, the uniformity of spreading powder decreases slightly due to the agglomeration

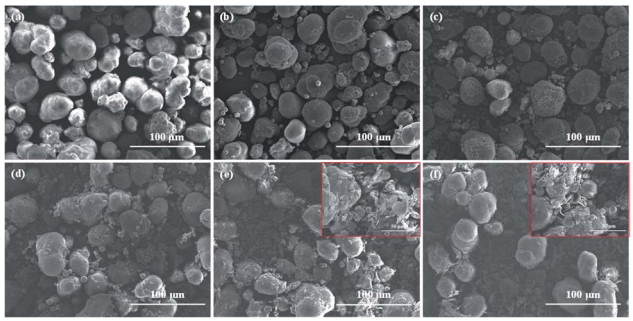

Fig. 4 SEM images of PA12/Al_2O_3 powder with different Al_2O_3 content: (a) 0 wt%, (b) 10 wt%, (c) 30 wt%, (d) 50 wt% and PA12/Al_2O_3/BN powder at (e) 40 wt% Al_2O_3 + 10wt% BN, (f) 30 wt% Al_2O_3 + 20wt% BN loading.

of a small number of Al_2O_3 particles. Following the introduction of the two-dimensional, layered BN, the spreading uniformity of the powder decreases substantially, particularly when the content of BN reaches 20 wt%, thus greatly reducing the PA12 composites' fluidity and increasing the likelihood of voids and defects during SLS processing. It can also be found from Fig. 4(e and f), the alignment of the BN plates tend to occur along the surface of Al_2O_3 particles, and can act as a bridge connecting the Al_2O_3 particles. This arrangement increases the contact area between BN and Al_2O_3, thus rendering it as conducive to the formation of dense thermal conductive networks.

Fig. 5(a–d) presents the cryo-fractured surface of the PA12/Al_2O_3 composites. It can be identified that the Al_2O_3 particles maintain consistent contact with the PA12 matrix. It is difficult, however, for Al_2O_3 to establish interconnected thermal networks, leading to low thermal conductivity. Pure PA12 exhibits a relatively smooth surface, while the PA12/Al_2O_3 composites show a rough fractured surface with the increase of Al_2O_3 loading. The toughness of the material is related to the roughness of the cross-section, meaning that it can be predicted that, with the increase of Al_2O_3 content, the crack resistance of the composites will gradually decrease.[26] As shown in Fig. 5(a), there exist a few voids on the surface of the pure PA12 sintered samples. When the Al_2O_3 loading increases to 50 wt%, the PA12

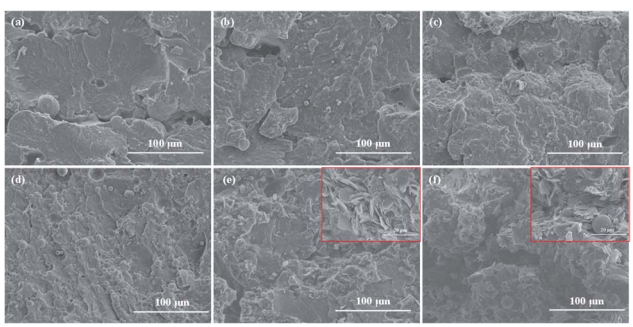

Fig. 5 SEM images of cryo-fractured surface of PA12/Al_2O_3 composites with different Al_2O_3 content: (a) 0 wt%, (b) 10 wt%, (c) 30 wt%, (d) 50wt% and PA12/Al_2O_3/BN composites at (e) 40 wt% Al_2O_3 + 10wt% BN, (f) 30 wt% Al_2O_3 + 20 wt% BN loading.

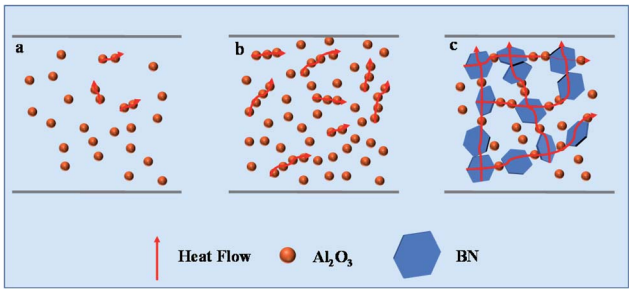

Fig. 6 Schematic illustration of thermal conduction paths in (a) PA12/Al_2O_3, (b) PA12/Al_2O_3 with higher content of Al_2O_3 and (c) PA12/Al_2O_3/BN composites.

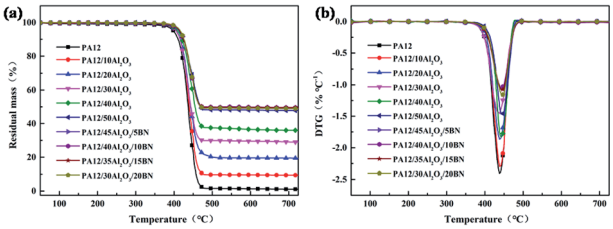

Fig. 7 (a) TGA and (b) DTG curves of pure PA12 and its composites.

Table 2 TGA data of pure PA12 and its composites[a]

Samples	T_5 (°C)	T_{max} (°C)	Residual mass (%)
PA12	399.04	438.71	1.12
PA12/10Al_2O_3	405.92	439.45	9.31
PA12/20Al_2O_3	405.78	439.73	19.32
PA12/30Al_2O_3	405.58	437.89	28.99
PA12/40Al_2O_3	409.32	443.86	35.94
PA12/50Al_2O_3	413.40	445.89	47.51
PA12/45Al_2O_3/5BN	415.11	443.52	48.89
PA12/40Al_2O_3/10BN	415.24	442.97	49.62
PA12/35Al_2O_3/15BN	415.24	444.74	49.60
PA12/30Al_2O_3/20BN	416.47	446.09	48.92

[a] T_5 is defined as the temperature of 5% weight loss; T_{max} is the temperature of the maximum mass loss rate; residual mass is the weight percentage of residue after TGA analysis.

powder is wholly melted by laser irradiation, forming almost no voids. This can be attributed to the fact that Al_2O_3 with a smaller particle size can fill the gaps between the PA12 matrix, and act as a heat source to facilitate heat transfer. This could explain the relatively high tensile strength of the sintered samples at high Al_2O_3 content. Fig. 5(e and f) shows the SEM images of the cryo-fractured surface of PA12/Al_2O_3/BN composites with different BN content. From these images, it can be noted that, while BN is predominantly arranging in a horizontal direction, there are nevertheless some fillers randomly distributed in the matrix, which a structure conducive to the formation of thermally conductive networks. Due to its two-dimensional layered structure, BN can act as a bridge connecting the Al_2O_3 particles, thus constructing more effective heat conduction paths. However, when the BN loading comes up to 20 wt%, numerous voids and defects were observed in the PA12/Al_2O_3/BN sintered parts, indicating weak interfacial interaction between BN and PA12. These voids and defects will consequently reduce the mechanical properties of the composites, rendering them as unsuitable for improving thermal conductivity.

Fig. 6 demonstrates the thermal conductivity improvement mechanism for PA12 composites, whereby the flakes represent BN, the small particles represent Al_2O_3 and the red lines represent possible heat conduction paths. As can be seen from Fig. 6(a), it is difficult for Al_2O_3 particles to contact and form thermal conduction paths at low content. With the increase of Al_2O_3 loading, the Al_2O_3 particles can connect to form a limited number of thermal conduction paths. However, the Al_2O_3 particles only connect *via* point-to-point contact, with large gaps remaining between some Al_2O_3 particles, therefore resulting in a large thermal interface resistance between the fillers and the PA12 matrix.[27] Once the BN has been added to the PA12/Al_2O_3 composites, the fillers tend to connect through point-to-surface contact and significantly increase the contact area of the filler/filler interface, resulting in a decrease of the interface thermal resistance and the formation of more effective thermally conductive paths. It can therefore be concluded that hybrid fillers enable the formation of effective heat conduction paths, especially when compared with PA12 composites that contain just one thermally conductive filler.

3.4. Thermal stability of composites

In order to study the effect of Al_2O_3 and BN content on the thermal stability of the PA12 composites, pure PA12 and its composites were heated from room temperature to 750 °C at a heating rate of 10 °C min^{-1} in a nitrogen atmosphere. In Fig. 7, which illustrates the TGA and derivative thermogravimetry (DTG) curves of pure PA12 and its composites, it is indicated that, with the increase of filler content, the residual mass of PA12 composites continues to grow. It is worth noting that the addition of fillers can slightly enhance the thermal stability of the PA12 composites, and delay the thermal degradation process compared to pure PA12. This enhancement could be ascribed to the fact that the fillers uniformly dispersed in the PA12 matrix act as a heat-resistant layer and mass transfer barrier, decreasing the degradation of composite materials. It can also be identified that all samples show similar thermal behaviour, indicating that the addition of fillers will not significantly change the degradation mechanism of the PA12 matrix. Table 2 lists the temperature of 5% weight loss (T_5) and the maximum mass loss rate (T_{max}). Obviously, the T_5 and T_{max} of each sample are slightly increased compared to those of pure PA12. This is due to the positive thermal stability of the fillers, in addition to the dense char layer formed as a result of the interaction between the fillers and the PA12 matrix during the thermal decomposition process, thus enhancing the thermal stability of the composites.

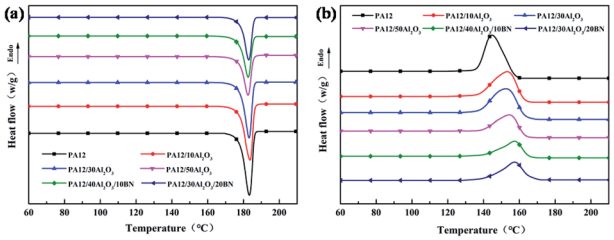

Fig. 8 DSC (a) heating and (b) cooling curves of pure PA12 and its composites.

Table 3 DSC data of pure PA12 and its composites

Samples	T_{ic} (°C)	T_{im} (°C)	Sintering window (°C)
PA12	157.2	178.3	21.1
PA12/10Al_2O_3	161.8	178.9	17.1
PA12/30Al_2O_3	161.6	179.1	17.5
PA12/50Al_2O_3	161.5	178.7	17.2
PA12/40Al_2O_3/10BN	164.1	178.4	14.3
PA12/30Al_2O_3/20BN	164.7	179.3	14.6

3.5. Melting and crystallisation behaviours of composites

The SLS sintering window is defined as the temperature gap between the initial melting temperature (T_{im}) and the initial crystallisation temperature (T_{ic}), which can be used to evaluate the processability of polymers.[28] Fig. 8 shows the differential scanning calorimetry (DSC) curves of pure PA12 and its composites. As can be seen from Fig. 8(a), the T_{im} of PA12 composites increases slightly with the increase of filler loading. This is chiefly due to the relatively strong interaction between the fillers and the matrix, which restricts the movement of the PA12 molecular chains, thereby increasing the T_{im}. Additionally, these powders demonstrate similar melting peaks during the heating process, while the T_{ic} of PA12 composites is much higher than pure PA12, with an increased peak width evident with the increase of filler content. This is because the filler has the ability to act as a nucleating agent, promoting the crystallisation of polymers during the process. Table 3 lists the sintering window of PA12 composites. When compared with pure PA12, the SLS sintering window of the PA12 composites is slightly narrowed. In order to avoid distortion and curling during the sintering process, the powder preheating temperature should be slightly higher than that of pure PA12.

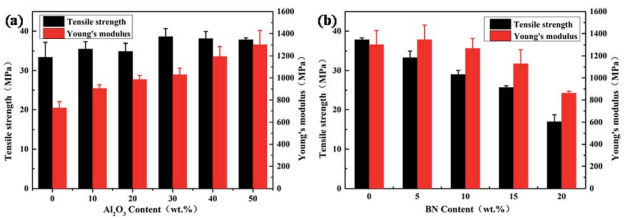

Fig. 9 Tensile properties of (a) PA12/Al_2O_3 and (b) PA12/Al_2O_3/BN (with total filler content of 50 wt%) sintered samples.

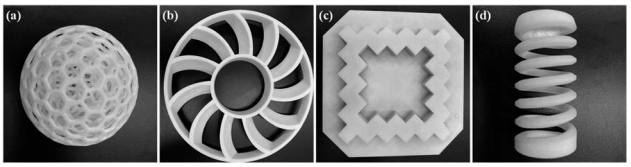

Fig. 10 Pictures of complex sintered parts produced by PA12 composites through selective laser sintering with different filler loading: (a) 10 wt% Al_2O_3, (b) 30 wt% Al_2O_3, (c) 50 wt% Al_2O_3, (d) 45 wt% Al_2O_3 + 5 wt% BN.

3.6. Mechanical properties of composites

In addition to thermal conductivity, mechanical properties are also considered an essential factor affecting the performance of thermally conductive composites. Fig. 9 shows the tensile strength and tensile modulus of the PA12 composites. It is worth noting that the addition of Al_2O_3 particles in the PA12 matrix is beneficial to enhance the mechanical properties. When the Al_2O_3 loading increases to 30 wt%, the tensile strength comes up to 38.6 ± 1.9 MPa, about 15% higher than that of pure PA12. In addition to this, the tensile modulus of the PA12 composites continues to grow with the increase of Al_2O_3 content. According to the Halpin–Tsai model, the tensile strength of the material is expected to be further improved by adding stronger fillers.[29] It is therefore projected to improve the mechanical properties of the materials with the addition of high-strength Al_2O_3 particles. In the meantime, the interface interaction between the matrix and the fillers will significantly affect the mechanical properties. The increase in the mechanical properties with the addition of Al_2O_3 indicates a positive interaction between the fillers and the PA12 matrix. It can be observed from Fig. 9(b) that, the tensile strength of the PA12 composites exhibits a notable decline with the augmentation of BN filler. In contrast, the decrease in tensile modulus is relatively slight, the reason being that the interaction between BN and the PA12 matrix is relatively weak, with the loose-packing of BN prone to the generation of defects and voids during the 3D printing process.

3.7. Complex sintered parts of composites

Fig. 10 demonstrates the PA12 composite parts alongside complex shapes fabricated by SLS technology. From these, it can be noted that they have a complete structure, absent of cracks or voids and with high dimensional accuracy, which indicates that SLS technology is useful in the preparation of high thermal conductivity composite materials with complex shapes.

4 Conclusions

In this study, the PA12/Al_2O_3/BN mixing powder consisting of features such as good fluidity and a wide sintering temperature range was successfully prepared. Through the two-step mixing approach, Al_2O_3 and BN were dispersed uniformly in the PA12 matrix, and then the obtained powder was successfully sintered into components with various shapes by laser irradiation. The thermal conductivity of the prepared PA12 composites reached

1.05 W m^{-1} K^{-1}, with 35 wt% Al_2O_3 and 15 wt% BN hybrid fillers, which was nearly 4 times of pure PA12. Moreover, the addition of Al_2O_3 particles and BN plates improved thermal stability and maintained the outstanding mechanical performance of the SLS prepared composites, displaying great potential in thermal management materials. It is thus foreseeable that selective laser sintering presents the opportunity for the utilisation of a brand-new approach in the preparation of functional parts consisting of high thermal conductivity and complex shapes.

Conflicts of interest

The authors declare no conflicts of interest.

Acknowledgements

This research was funded by the joint research project "Research and Development of New Functional Polymer Materials Based on Additive Manufacturing" between Oechsler Plastic Products (Taicang) Co., Ltd. and East China University of Science and Technology, project number: D900-81802.

Notes and references

1 B. Fan, Y. Liu, D. He and J. Bai, Enhanced thermal conductivity for mesophase pitch-based carbon fiber/modified boron nitride/epoxy composites, *Polymer*, 2017, **122**, 71–76.

2 J. Hu, Y. Huang, Y. Yao, G. Pan, J. Sun, X. Zeng, R. Sun, J. B. Xu, B. Song and C. P. Wong, Polymer Composite with Improved Thermal Conductivity by Constructing a Hierarchically Ordered Three-Dimensional Interconnected Network of BN, *ACS Appl. Mater. Interfaces*, 2017, **9**(15), 13544–13553.

3 Z. B. Zhao, L. Tai, D. M. Zhang, Z. F. Wang and Y. Jiang, Preparation of poly(octadecyl methacrylate)/silica-(3-methacryloxypropyl trimethoxysilane)/silica multi-layer core–shell nanocomposite with thermostable hydrophobicity and good viscosity break property, *Chem. Eng. J.*, 2017, **307**, 891–896.

4 Z. Liu, J. Li and X. Liu, Novel Functionalized BN Nanosheets/Epoxy Composites with Advanced Thermal Conductivity and Mechanical Properties, *ACS Appl. Mater. Interfaces*, 2020, **12**(5), 6503–6515.

5 N. G. Sahoo, H. K. F. Cheng, J. Cai, L. Li, S. H. Chan, J. Zhao and S. Yu, Improvement of mechanical and thermal properties of carbon nanotube composites through nanotube functionalization and processing methods, *Mater. Chem. Phys.*, 2009, **117**(1), 313–320.

6 G. V. Salmoria, R. A. Paggi, A. Lago and V. E. Beal, Microstructural and mechanical characterization of PA12/MWCNTs nanocomposite manufactured by selective laser sintering, *Polym. Test.*, 2011, **30**(6), 611–615.

7 R. A. Paggi, V. E. Beal and G. V. Salmoria, Process optimization for PA12/MWCNT nanocomposite manufacturing by selective laser sintering, *Int. J. Adv. Des. Manuf. Technol.*, 2012, **66**(9–12), 1977–1985.

8 S. R. Athreya, K. Kalaitzidou and S. Das, Microstructure, thermomechanical properties, and electrical conductivity of carbon black-filled nylon-12 nanocomposites prepared by selective laser sintering, *Polym. Eng. Sci.*, 2012, **52**(1), 12–20.

9 L. Lanzl, K. Wudy, S. Greiner and D. Drummer, Selective Laser Sintering of Copper Filled Polyamide 12: Characterization of Powder Properties and Process Behavior, *Polym. Compos.*, 2019, **40**(5), 1801–1809.

10 R. Hong, Z. Zhao, J. Leng, J. Wu and J. Zhang, Two-step approach based on selective laser sintering for high performance carbon black/polyamide 12 composite with 3D segregated conductive network, *Composites, Part B*, 2019, **176**, 107214.

11 C. Yan, L. Hao, L. Xu and Y. Shi, Preparation, characterisation and processing of carbon fibre/polyamide-12 composites for selective laser sintering, *Compos. Sci. Technol.*, 2011, **71**(16), 1834–1841.

12 P. Chen, H. Wu, W. Zhu, L. Yang, Z. Li, C. Yan, S. Wen and Y. Shi, Investigation into the processability, recyclability and crystalline structure of selective laser sintered Polyamide 6 in comparison with Polyamide 12, *Polym. Test.*, 2018, **69**, 366–374.

13 C. Yan, Y. Shi, J. Yang and J. Liu, Preparation and selective laser sintering of nylon-12 coated metal powders and post processing, *J. Mater. Process. Technol.*, 2009, **209**(17), 5785–5792.

14 Y. Lu, L. Wang and Y. Chen, Solid-state shear milling method to prepare PA12/boron nitride thermal conductive composite powders and their selective laser sintering 3D-printing, *J. Appl. Polym. Sci.*, 2020, **137**(23), 48766.

15 S. Yuan, Y. Zheng, C. K. Chua, Q. Yan and K. Zhou, Electrical and thermal conductivities of MWCNT/polymer composites fabricated by selective laser sintering, *Composites, Part A*, 2018, **105**, 203–213.

16 V. D. Mai, D. I. Lee, J. H. Park and D. S. Lee, Rheological Properties and Thermal Conductivity of Epoxy Resins Filled with a Mixture of Alumina and Boron Nitride, *Polymers*, 2019, **11**(4), 597.

17 Y. Chen, X. Hou, M. Liao, W. Dai, Z. Wang, C. Yan, H. Li, C.-T. Lin, N. Jiang and J. Yu, Constructing a "pea-pod-like" alumina–graphene binary architecture for enhancing thermal conductivity of epoxy composite, *Chem. Eng. J.*, 2020, **381**, 122690.

18 Y. Wang, W. Wu, D. Drummer, C. Liu, W. Shen, F. Tomiak, K. Schneider, X. Liu and Q. Chen, Highly thermally conductive polybenzoxazine composites based on boron nitride flakes deposited with copper particles, *Mater. Des.*, 2020, **191**, 108759.

19 H. Wang, L. Li, Y. Chen, M. Li, H. Fu, X. Hou, X. Wu, C. T. Lin, N. Jiang and J. Yu, Efficient Thermal Transport Highway Construction Within Epoxy Matrix via Hybrid Carbon Fibers and Alumina Particles, *ACS Omega*, 2020, **5**(2), 1170–1177.

20 Z. Ghezelbash, D. Ashouri, S. Mousavian, A. H. Ghandi and Y. Rahnama, Surface modified Al_2O_3 in fluorinated polyimide/Al_2O_3 nanocomposites: Synthesis and characterization, *Bull. Mater. Sci.*, 2012, **35**(6), 925–931.

21 Y.-K. Kim, J.-Y. Chung, J.-G. Lee, Y.-K. Baek and P.-W. Shin, Synergistic effect of spherical Al_2O_3 particles and BN nanoplates on the thermal transport properties of polymer composites, *Composites, Part A*, 2017, **98**, 184–191.

22 J. P. Cheng, T. Liu, J. Zhang, B. B. Wang, J. Ying, F. Liu and X. B. Zhang, Influence of phase and morphology on thermal conductivity of alumina particle/silicone rubber composites, *Appl. Phys. A: Solids Surf.*, 2014, **117**(4), 1985–1992.

23 G. Y. Duan, Y. Wang, J. R. Yu, J. Zhu and Z. M. Hu, Improved thermal conductivity and dielectric properties of flexible PMIA composites with modified micro- and nano-sized hexagonal boron nitride, *Front. Mater. Sci.*, 2019, **13**(1), 64–76.

24 R. D. Goodridge, C. J. Tuck and R. J. M. Hague, Laser sintering of polyamides and other polymers, *Prog. Mater. Sci.*, 2012, **57**(2), 229–267.

25 T. Pozar, J. Lalos, A. Babnik, R. Petkovsek, M. Bethune-Waddell, K. J. Chau, G. V. B. Lukasievicz and N. G. C. Astrath, Isolated detection of elastic waves driven by the momentum of light, *Nat. Commun.*, 2018, **9**, DOI: 10.1038/s41467-018-05706-3.

26 C. E. Y. Erpek, G. Ozkoc and U. Yilmazer, Effects of Halloysite Nanotubes on the Performance of Plasticized Poly(Lactic Acid)-Based Composites, *Polym. Compos.*, 2016, **37**(11), 3134–3148.

27 Z. Li, D. Ju, L. Han and L. Dong, Formation of more efficient thermally conductive pathways due to the synergistic effect of boron nitride and alumina in poly(3-hydroxylbutyrate), *Thermochim. Acta*, 2017, **652**, 9–16.

28 M. Vasquez, B. Haworth and N. Hopkinson, Methods for quantifying the stable sintering region in laser sintered polyamide-12, *Polym. Eng. Sci.*, 2013, **53**, 1230–1240.

29 Y. Zare, Development of Halpin–Tsai model for polymer nanocomposites assuming interphase properties and nanofiller size, *Polym. Test.*, 2016, **51**, 69–73.